Low-cost and High Performance Optical Fiber-based Sensor for Liquid Level Monitoring

Joana Martins, Camilo Rodriguez, Fátima Domingues, Rute A. S. Ferreira, Paulo Antunes, Paulo S. André, Senior Member, IEEE

Abstract— **Liquid level sensing is nowadays a relevant issue in a broad range of applications, forcing the sensors performance and cost to be evaluated in parallel. This work proposes a fiber optic-based liquid level sensor system using a Fabry-Pérot interferometer (FPI) embedded into a polyurethane resin diaphragm. The FPI is based on microcavities generated upon catastrophic fuse effect, enabling the fiber recycling and sensors fabrication in a cost-effective way, compared to traditional methods. To enable the simultaneous temperature control, a Fiber Bragg Grating was used as thermal reference sensor to compensate the temperature cross-sensitivity. The sensor prototype was tested in a field application, using two different configurations, an open chamber configuration, where the diaphragm is in contact with the atmosphere, and a closed chamber configuration, revealing sensitivities of 4.4±0.1 pm/mm and 1.57 ± 0.04, respectively. These sensitivity values are within the figures of merit for diaphragm-based sensors recently reported.**

Index Terms— *Liquid level, Fabry-Pérot, Fiber Fuse Effect, Diaphragm, Strain, Temperature.*

I. INTRODUCTION

NOWADAYS, the monitoring of the liquid-air interface is required to infer level in a wide variety of applications such as, for instance, fuel supply systems, oil reservoirs, wastewater treatment plants [1]. Other relevant applications can be found in medical treatments, chemical processing and pharmaceutical development, demanding high resolution on liquid level detection [2]. Traditionally, liquid level sensing is mainly based on mechanic and electrical techniques, such as capacitance and radio frequency admittance [3], float type devices as magnetic floating gauge [4], ultrasonic and radar based sensing [3]. Despite that electrical-based sensors are widely employed, their applicability is limited when the sensing medium is conductive, potentially explosive and erosive [5], [6].

Optical fiber-based sensors have been considered an attractive prospect for liquid level monitoring, due to its unique advantages, such as electromagnetic immunity, electrical insulation, compatibility with remote sensing and sensor multiplexing. Moreover, these advantages render optical fiber appropriate for long term, reliable level measurements in special conditions [7]–[9]. Distinct operation principles are behind optical-based sensing, namely refractive index variation. These sensors measure the liquid level based on the immersed sensor length which lead to a specific effective surrounding refractive index and several implementation examples can be found: etched Fiber Bragg Grating (FBG) [6], etched chirped FBG [2] or long period grating (LPG) [10]. An additional technology is based on excessively tilted FBG that generates a fast and slow-axis due to its birefringence [11]. However, due to its length ($\sim 10^{-2}$ m), these sensors are restricted to a reduced range liquid measurement.

Fiber Mach-Zehnder modal interferometers are also used to detect liquid level, as the medium in the interferometer surroundings induces an optical phase difference between the core and cladding modes. Several configurations have been suggested, such as: i) to splice a segment of no-core multimode fiber with a single mode fiber (SMF)[12]; ii) to splice a segment of stripped thin core SMF between two standard SMFs [13]; iii) or place a SMF section between two up-tapers (resulted from fusion splices), acting as beam-splitter and beam combiner [14]. Depending on the sensing range that is required for a specific application, the length of the fiber segments used to assemble the interferometer can be tailored. Though, these sensors reveal sensitivity values that decrease with the FBG dimension, as shown by the Wen *et al.* reporting sensitivities of 0.19 nm/m and 22.5 nm/m for a FBG with length of 10.0 m and 14.3 cm, respectively [14].

Diaphragm-based extrinsic Fabry-Pérot-based sensors are another common interferometric configuration to sense liquid

J. M. is with the Department of Physics, CICECO – Aveiro Institute of Materials, and Instituto de Telecomunicações, University of Aveiro, 3810-193 Aveiro, Portugal (costa.joana@ua.pt).

C. R. is with Federal University of Espírito Santo, Department of Electrical Engineering, Av. Fernando Ferrari, 514, Goiabeiras, Vitória 29075-910, Brazil (camiloard@gmail.com);

F.R. is with Instituto de Telecomunicações, University of Aveiro, 3810-193 Aveiro, Portugal (fdomingues@av.it.pt).

R. A. S. F. is with Department of Physics, CICECO – Aveiro Institute of Materials, University of Aveiro, 3810-193 Aveiro, Portugal (rferreira@ua.pt).

P. A. is with Department of Physics, I3N and Instituto de Telecomunicações, University of Aveiro, 3810-193 Aveiro, Portugal (pantunes@ua.pt).

P. S. A. is with Instituto de Telecomunicações, University of Aveiro, 3810-193 Aveiro, Portugal and with the Department of Electrical and Computer Engineering, Instituto Superior Técnico, University of Lisbon, 1049-001 Lisbon, Portugal (paulo.andre@lx.it.pt).

level. In this case, liquid level is sensed through hydrostatic pressure which induces a diaphragm deflection, changing the Fabry-Pérot cavity length. Some of the reported designs include an elastic silicon diaphragm connected to the fiber tip [15], three-layer arrangement diaphragm of polyimide, metal and epoxy-based negative photoresist linked to the fiber tip by a glass tube [16] and a thin silica diaphragm attached to the fiber end-face by a fused-silica ferrule [17]. Despite being applicable for long range liquid measurements, these sensors often present optical alignment instability [16].

The FBGs are amongst the most used technology for liquid level sensing solutions, in which FBG can be mounted in a cantilever, for instance, in a polypropylene [5] or an high elastic steel bending cantilever [18], both fixed to a column buoy that transfers liquid level variations into vertical pressure. FBG can also sense liquid level through hydrostatic pressure, but bare FBG shows poor sensitivity to pressure variations (~0.003 pm/kPa) [19]. However, this negative aspect may be overcome by incorporating FBG in diaphragms, or even in polymer casings. Some of the proposed methods consist in bonding the FBG to the surface of a stainless-steel diaphragm [9], an elastic metal film [20] or a single sheet graphene [21]. Alternatively, FBG may be embedded in a polymer-field aluminum casing [22], a two different polymers (polycarbonate and polytetrafluoroethylene) cube [23], a silicon rubber cylinder [24], or in diaphragms made of epoxy resin [1] or carbon fiber composite [25]. These sensors are suitable for long range continuous liquid measurements, easily constructed and report appreciable sensitivities to level change. Moreover, the sensitivities are not length or surrounding refractive index dependent. Additionally, diaphragm based sensors exhibit higher mechanical resistance, as they protect the optical fiber from direct contact with liquid, increasing the sensor lifetime [1], [22], [25].

Fiber Fabry-Pérot intrinsic interferometers (FPI) are also an alternative optical spectral based technology, able to be used in optical fiber sensing applications, with most of the FBGs advantages. Those interferometers have shown higher strain sensitivity (2.56 pm/µε)[26] compared to FBGs (1.2 pm/µε)[27], and when embedded into a polymer casing presents a pressure sensitivity of 13.67 pm/kPa [28], while embed FBG in similar conditions yields 8.7 pm/kPa of pressure sensitivity [22]. This sensitivity enhancement supports the use of FPI for liquid level monitoring, which can be produced by chemical etching [29], micromachining [30], and optical fiber splicing [31], [32]. However, these operations require high economical investments or complex implementations.

In this work, we present a novel and cost-effective solution, able to monitor liquid level, based on microcavities produced using recycled optical fibers, destroyed by the catastrophic fuse effect. The sensor is assembled by embedding the FPI into a polyurethane epoxy diaphragm. Comparing with other sensors, this design can be applied to wide range – high sensitivity measurements, with simple and low-cost implementation.

This paper is organized as follows. Section 2 presents the operating principle, the sensor design and the mathematical model. Section 3 describes the experimental setup used to evaluate the proposed sensor response. In section 4 the results are presented and finally, the main conclusions are drawn in section 5.

II. OPERATION PRINCIPLE AND SENSOR DESIGN

A Fabry-Pérot interferometer can be described as a cavity between two reflecting surfaces. The phase shift of a propagating optical signal after a round trip propagation in the interferometer cavity, ϕ_{FPI}, is given by:

$$\phi_{FPI} = \frac{4\pi}{\lambda} nl \qquad (1)$$

where l is the cavity physical length, λ is the optical signal wavelength, and n represents the cavity refractive index [33].

The interference between both signals, incident and after a roundtrip, imposes in a periodic modulated optical reflection spectrum, which is well described by a square cosine function. The constructive and destructive interference correspond to the maximum and minimum of the spectra and are described by $\phi_{FPI} = 2m\pi$ and $\phi_{FPI} = (2m + 1)\pi$, respectively, where m is the interference order [34]. When a physical perturbation, such as longitudinal strain, induces a cavity physical length change, the FPI reflection spectrum shifts according to:

$$\Delta\lambda_{min} = \frac{4}{2m + 1} \Delta l \qquad (2)$$

where $\Delta\lambda_{min}$ is the mth interference minimum wavelength shift of the reflection optical spectra and Δl is the cavity physical length change.

The production of this liquid level sensor was divided in two stages. In the first one, a SMF was destroyed by the catastrophic fuse effect and afterwards spliced to another one to obtain a microcavity with dimensions suitable for the FPI operation. In the second stage, the FPI was embedded into a liquid epoxy resin that, after cure, forms a cylindrical diaphragm with a 1.6×10^{-3} m thickness wall and 5.0×10^{-2} m mm diameter (the FPI was located in the diaphragm central position).

The catastrophic fuse effect is a fiber self-induced destruction phenomenon triggered by a local heating point, commonly in a damaged connector, in a dirty connector or in a fiber tight bend. This phenomenon is characterized by the propagation of a fuse plasma region towards the optical source, leaving behind a periodic void sequence with dimensions and spatial period in the order of micrometres. After the catastrophic fuse effect, the optical fiber is no longer suitable for signal transmission [35].

To induce the catastrophic fuse effect, it was followed procedure describe in detail in [36]. A Raman fiber laser (IPG, model RLR-10-1480) was used to generate a 3.0 W optical signal with a wavelength of 1480 nm. This optical signal was injected into a SMF (SMF28- Corning). The fiber end was placed in contact with a metallic foil to ignite the fuse effect.

Fig. 1A. shows the generated voids in the fiber core. This damaged fiber was cleaved and then spliced to a SMF, using a splicing machine (Fujikura, model FSM-040S). As a result, a large dimension void was formed in the splice region, as shown in Fig. 1B. Then the fiber was cleaved in the splice region, intersecting the large void, in order to obtain a fiber end tip structure presented in Fig 1C. The final step of the FPI production, Fig 1D, was splicing the cleaved fiber end tip to a SMF.
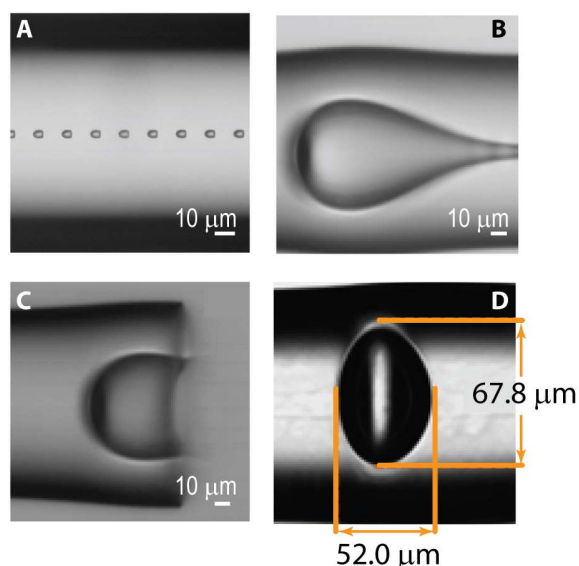
Fig. 1. Optical microscopy images of the optical fiber during the FPI formation procedure. (A) general view of several voids in a damaged fiber by the catastrophic fuse effect; (B) large dimension void after the first splice with SMF (C) end tip after cleaving and the (D) FFPI.

To embed the cavity into the epoxy, we followed a similar process to the reported in [1]. First, the acrylate protection was removed around 20 mm in the FPI section, to promote the adhesion between the epoxy resin to the fiber. Afterward, the fiber was pre-stressed in a container (plastic cast), and the epoxy resin (Liquid lens – Advanced 2) applied, keeping the cast undisturbed for 24 hours. Figure 2 show the sensor head components and the final assembly.
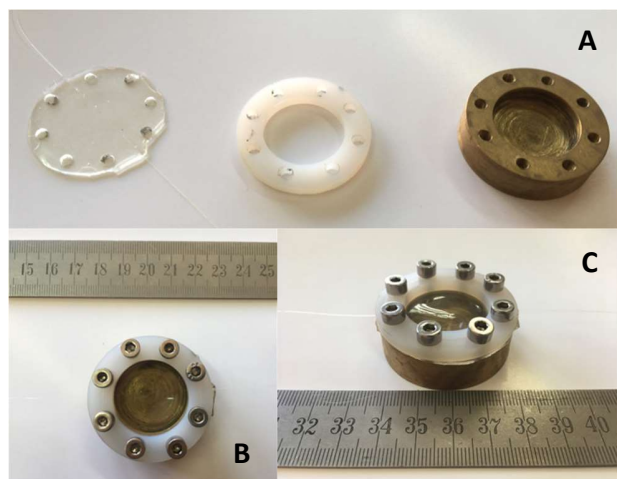
Fig. 2. Photography of the sensor head. (A) Components, from left to right, epoxy membrane with the embedded FPI, PTFE O-ring and metallic chamber; (B and C) Final assembled sensor head.

Besides longitudinal strain, the temperature change can also induce the change in the cavity length, due to material thermal expansion, leading to cross-sensitivity effect between the strain and temperature. In order to decouple the temperature and strain effects on the FPI response, a FBG-based temperature sensor was placed near the diaphragm. This FBG was recorded in a

photosensitive optical fiber (FiberCore PS1250/1500) using the phase mask technique with a KrF UV Excimer laser emitting at 248 nm (BraggStar Industrial model from Coherent). The fiber was exposed during 30 seconds to 5×10^{-3} J energy pulses with a repetition frequency of 500 Hz.

Both the influence of temperature (ΔT) and level variation (ΔL) on one of the FPI interference minimum wavelength and on the FBG Bragg wavelength are determined by the matrix:

$$\begin{bmatrix} \lambda_{FFPI} \\ \lambda_{FBG} \end{bmatrix} = \begin{bmatrix} k_{L,FFPI} & k_{T,FFPI} \\ k_{L,FBG} & k_{T,FBG} \end{bmatrix} \begin{bmatrix} \Delta L \\ \Delta T \end{bmatrix} + \begin{bmatrix} \lambda_{0,FFPI} \\ \lambda_{0,FBG} \end{bmatrix} \qquad (3)$$

where $k_{L,FFPI}$ and $k_{L,FBG}$ is the FPI and FBG level sensitivity, $k_{T,FFPI}$ and $k_{T,FBG}$ the FPI and FBG temperature sensitivity and $\lambda_{0,FFPI}$ and $\lambda_{0,FBG}$ the unperturbed FPI destructive interference wavelength and Bragg wavelength measured, respectively. Compared with the common FBG temperature sensitivity (≈ 10 pm/°C at 1550 nm)[27] , the common FBG level (pressure) sensitivity (3.1×10^{-5} pm/mm)[19] can be neglected for typical operation range ($k_{L,FBG} = 0$).

III. EXPERIMENTAL SETUP

A. Diaphragm Thermal Characterization

To determine the sensor temperature sensitivity, $k_{T,FFPI}$, the characterization was performed using a thermal chamber (Challenge Angelantoni Industrie, Model 340). The temperature was increased from 5°C to 40°C with 5°C steps. With temperature stabilization time of 30 minutes in each step, the reflection optical spectra were acquired using an interrogator (Micron Optics, Model SM 125-500. The same procedure was used to estimate the FBG thermal sensitivity, $k_{T,FBG}$.

B. Liquid Level Measurements

The liquid level measurements were performed using an acrylic tank with a 16.5 cm side square base and 96 cm height. The sensor was tested using two different configurations, as shown in Fig. 3.
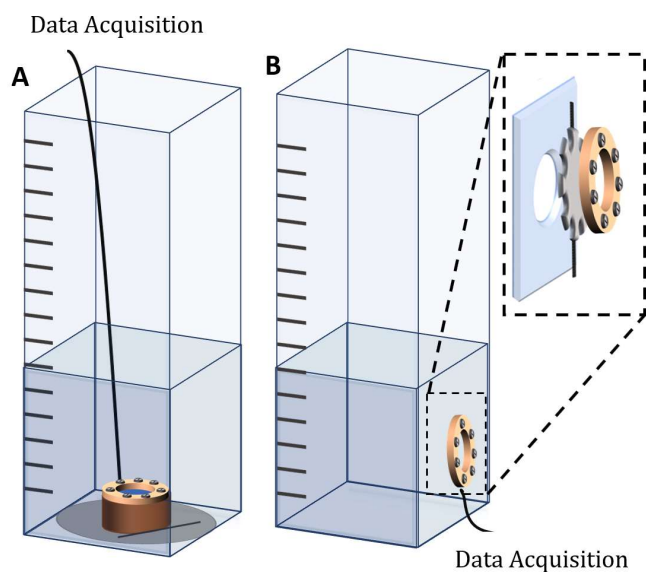
Fig. 3. Schematics of the used configurations for the liquid level measurements; (A) closed chamber, with the FPI at the tank bottom, and (B) open chamber, with the FPI at the tank sidewall.

Fig. 4. Scheme highlighting pressure gradients in (A,B) closed and (C) open chamber configurations. The zero level case, where the pressure gradient is null in both configurations, the chamber is at atmospheric pressure (P_{atm}).In the presence of the liquid, the pressure gradient is smaller in closed chamber configuration, because under applied pressure (P_{liq}) the chamber internal pressure increases (P_{int}) while in open chamber configuration it is constant (P_{atm}).

In the closed chamber configuration, the diaphragm is placed into the sensor holder between a brass metal chamber and a polytetrafluoroethylene (PTFE) ring, as shown in Fig. 3. Thereafter, the sensor support was placed at the tank bottom (Fig. 3A.)

The PTFE ring (2.6×10^{-2} m internal diameter; 4.5×10^{-2} m external diameter), allows the diaphragm direct contact with the surrounding medium and the metallic chamber has a central cylindrical cavity (3.7×10^{-3} m depth), to where the diaphragm deflection is possible. To ensure that the diaphragm lays flat and does not bend, eight open holes were cut in the diaphragm for the eight screws that tighten all parts. In the open chamber configuration, the diaphragm and the PTFE ring were attached to a circular aperture in the tank sidewall (3B). In both configurations, the FBG (temperature sensor) was placed at the tank bottom, enclosed in a metal tube to be isolated from the liquid vibration. Water was used as sensed medium. The reflection optical spectra of both FBG and FPI were acquired from 0 to 90×10^{-2} m water level, with a step of 2×10^{-2} m. Data was collected using the afore mentioned interrogator during level rise and fall. A hose connected to the tap water was used to fill the tank and the tank valve to drain it.

While sensing, it is important to notice the difference between pressure gradients in each configuration, as illustrated in Fig 4. In the closed chamber configuration, the diaphragm is placed on top of the closed chamber (3.7×10^{-3} m mm depth) and as the liquid level increase, the diaphragm deflects towards this air-filled chamber, increasing the internal pressure (P_{int}), which restrains the diaphragm deflection. On the open chamber configuration, the diaphragm deflects freely due to the pressure gradient between the liquid and the atmospheric pressure (P_{atm}).

IV. RESULTS

Fig. 5. displays the FBG and FPI reflection optical spectra at different temperatures, showing, in both cases, a shift towards longer wavelengths as temperature rises. As expected, with temperature increase, the FBG grating expands and the thermo-optic effect induces a change in the effective refractive index leading to a shift in the Bragg wavelength. As for the FFPI, the diaphragm also extends due to temperature increase, inducing a deformation in the embedded optical fiber, resulting in the expansion of the FPI cavity and a shift of the optical reflection spectra.
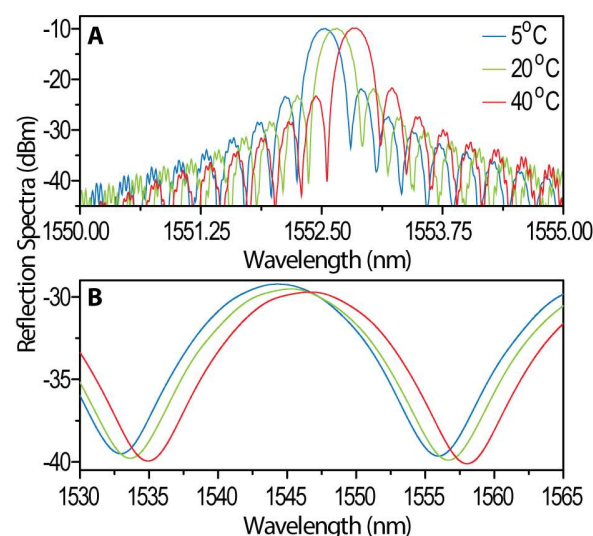
Fig. 5. FBG (A) and FFPI (B) reflection optical spectra measured at 5, 20 and 40°C.

Fig 6. and Fig 7. displays the reflected optical spectral shift as function of the temperature for the FBG and FPI sensor, respectively. For the FFPI sensor, λ is given by the interference minimum tracking at the wavelength range [1530, 1535] nm, while in the FBG this is given by the Bragg wavelength tracking. Both functions reveal a linear dependence. From the data best linear fit (Fig. 6 and Fig. 7), the FBG ($k_{T,FBG}$) and the FFPI ($k_{T,FFPI}$) thermal sensitivities were estimated as 8.6 ±0.3 pm/°C and 61±4 pm/°C, respectively.
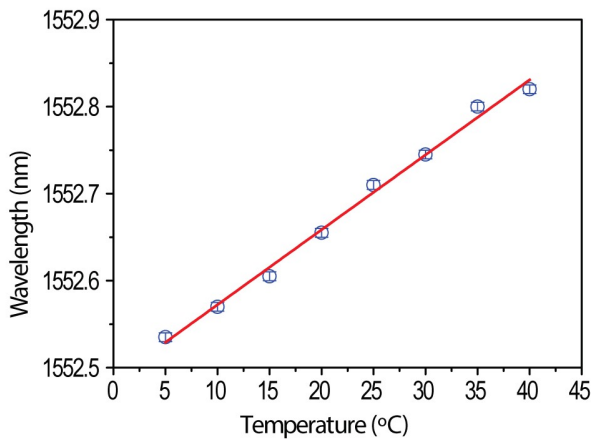
Fig. 6. FBG Bragg wavelength shift as function of the temperature. The line is the data best linear fit (r^2>0.99).
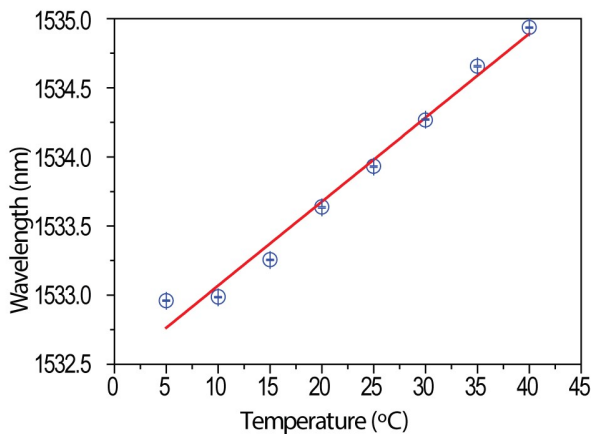
Fig. 7. FFPI reflected optical spectral shift as function of the temperature. The line is the data best linear fit (r^2>0.97).

Fig 8. displays the wavelength of the FPI interference minimum at the [1530,1536] wavelength range, as function of the liquid level variation, using both configurations (closed and open chamber) during level rise and fall. The temperature variation was monitored by the FBG.
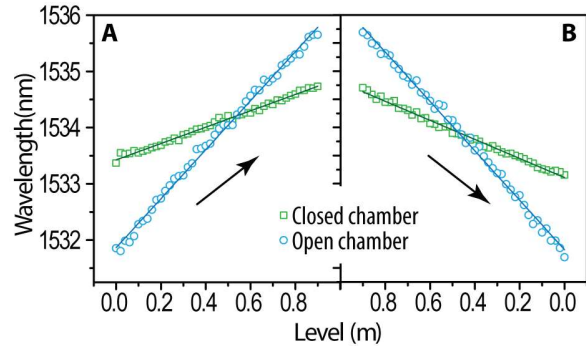
Fig. 8. FPI interference minimum wavelength as function of the level variation in closed chamber configuration (green circles) and open chamber configuration (blue circles), during level rise (left) and level fall (right), as indicated by the arrows. The lines are the data bet linear fits (r^2>0.99).

As predicted, the optical spectra shift towards longer wavelengths (during level rise) due to the strain induced by the water hydrostatic pressure. During level fall, the return to the original spectral position is observed (when the diaphragm is at a pressure free state). The sensor figures of merit are shown in Table I, revealing analogous sensitivities within the error as the level rises and falls, in the open chamber configuration, while in closed chamber configuration, there is a disparity between the level and rise sensitivities, that could be related with the elasticity of the diaphragm membrane.

TABLE I
LEVEL RISE AND LEVEL FALL SENSITIVITIES OF CLOSED AND OPEN CHAMBER CONFIGURATIONS

Close chamber	$k_{L,FFPI}$ (pm/mm)
Level Rise	1.45±0.02
Level Fall	1.69±0.02
Open chamber	
Level Rise	4.35±0.05
Level Fall	4.39±0.05

The FPI in open chamber configuration proves to be more sensitive than in closed chamber configuration, which means that, in the first configuration, there is a greater diaphragm deflection than in the latter one. Considering the mean values of table I, the level sensitivity was estimated as 1.57 ± 0.04 pm/mm and 4.4 ±0.1 pm/mm for open and closed chamber configuration, respectively. These results are in good agreement with the expected ones from the theoretical models. As mentioned in Section II, in the closed chamber configuration, under applied pressure (liquid level) the diaphragm deflects towards the chamber, increasing the internal pressure, which restrains the diaphragm deflection, since the pressure gradient between both sides of the diaphragm is reduced. Otherwise, in the open chamber configuration the diaphragm is in direct contact with the atmosphere, the pressure gradient increases and without any constriction, the diaphragm deflects widely.

Comparing with other sensors based on similar technology, the proposed sensor presents higher sensitivity and an operation range within the ranges commonly reported, as demonstrated in Table II. This higher sensitivity is reached using an FPI which is more sensitive to strain than the commonly used FBG.

Additionally, using polyurethane resin, which is a malleable material, and mold it as a diaphragm it allows a higher deflection in response to the increasing liquid boosting the sensor performance. The possibility to tailor the sensitivity, by setting the sensor configuration, provide an additional degree of flexibility in the sensor design as function of the operational dynamic range.

TABLE II
SENSITIVITIES AND RANGE OPERATION OF
FIBER OPTIC LEVEL SENSORS BASED ON DIFFERENT TECHNOLOGIES.

Technology	Pressure Sensitivity (pm/kPa)	Pressure Range (kPa)	Level Sensitivity (pm/mm)	Level Range (mm)
FFPI embed polyurethane diaphragm	449	8.3	4.4	900
FBG embed polycarbonate and polytetrafluoroethylene[23]	0.81	10^4	-	-
FBG embed in silicon-based rubber [22]	8.7	482.6	-	-
FBG in cantilever [5]	-	-	15	400
FBG embed in carbon fiber composite [25]	-	-	0.185	10000
FBG attached to stainless steel diaphragm [9]	1.75	10^3	-	-
Fiber modal interferometer [14]	-	-	[0.19-22.5]	[10000-143]
FBG embed in polymer [24]	-	-	2.3	100
Open cavity FFPI [33]	470± 30	8	-	-
FBG in POF embed in epoxy resin [37]	-	-	5.72 ± 0.04	750
Etched chirped FBG [2]	-	-	1214	7
FBG attached to single sheet graphene diaphragm [21]	-	-	2.48	1000
FBG embed in epoxy resin d[1]	-	-	2.74	500
FFPI embed in epoxy resin [28]	59.39	900	-	-

V. CONCLUSIONS

In this work, we presented the development of a temperature compensated liquid-level sensor based on a FPI embedded in polyurethane resin, using a cost-effective method for the FPI production by recycling of optical fiber destroyed by the catastrophic fuse effect. The sensor prototype was tested in two different configurations, revealing maximum sensitivities of 1.57 ± 0.04 pm/mm and 4.4 ±0.1 pm/mm, which is within the range of other diaphragm sensors recently reported in the literature. Since both polyurethane resin and PTFE are resistant and enduring materials, this sensor can be successfully used in harsh environments, such as chemical processing, fuel storage and oil reservoirs applications. Due to its temperature correction, this configuration is also suitable in non-temperature controlled applications.

REFERENCES

[1] C. A. R. Díaz, A. G. Leal-Junior, P. S. B. Andre, P. F. C. Antunes, M. J. Pontes, A. F. Neto, and M. R. N. Ribeiro, "Liquid Level Measurement based on FBG-embedded Diaphragms with Temperature Compensation," *IEEE Sens. J.*, vol. 18, no. 1, pp. 193–200, 2017.

[2] H. Y. Chang, Y. C. Chang, H. J. Sheng, M. Y. Fu, W. F. Liu, and R. Kashyap, "An ultra-sensitive liquid-level indicator based on an etched chirped-fiber bragg grating," *IEEE Photonics Technol. Lett.*, vol. 28, no. 3, pp. 268–271, 2016.

[3] B. G. Liptak, *Instrument Engineers' Handbook, Volume One: Process Measurement and Analysis*, 4th ed. CRC Press, 2003.

[4] D. R. Gillum, *Industrial Pressure, Level and Density Measurement*, 2nd ed. ISA, 2009.

[5] K. R. Sohn and J. H. Shim, "Liquid-level monitoring sensor systems using fiber Bragg grating embedded in cantilever," *Sensors Actuators, A Phys.*, vol. 152, no. 2, pp. 248–251, 2009.

[6] B. Yun, N. Chen, and Y. Cui, "Highly sensitive liquid-level sensor based on etched fiber bragg grating," *IEEE Photonics Technol. Lett.*, vol. 19, no. 21, pp. 1747–1749, 2007.

[7] K. T. V. Grattan and T. Sun, "Fiber optic sensor technology: an overview.," *Sensors Actuators, A Phys. A Phys.*, vol. 82, no. 1, pp. 40–61, 2000.

[8] B. Culshaw, "Optical Fibre Sensors : a Current Perspective," *Open Opt. J.*, vol. 7, no. 1, pp. 21–31, 2013.

[9] J. Huang, Z. Zhou, X. Wen, and D. Zhang, "A diaphragm-type fiber Bragg grating pressure sensor with temperature compensation," *Meas. J. Int. Meas. Confed.*, vol. 46, no. 3, pp. 1041–1046, 2013.

[10] S. Khaliq, S. W. James, and R. P. Tatam, "Fiber-optic liquid-level sensor using a long-period grating," *Opt. Lett.*, vol. 26, no. 16, pp. 1224–1226, 2001.

[11] C. Mou, K. Zhou, Z. Yan, H. Fu, and L. Zhang, "Liquid level sensor based on an excessively tilted fibre grating," *Opt. Commun.*, vol. 305, pp. 271–275, 2013.

[12] J. E. Antonio-Lopez, J. J. Sanchez-Mondragon, P. LiKamWa, and D. A. May-Arrioja, "Fiber-optic sensor for liquid level measurement," *Opt. Lett.*, vol. 36, no. 17, p. 3425, 2011.

[13] B. Xu, J. Q. Li, Y. Li, and X. Y. Dong, "A thin-core fiber modal interferometer for liquid-level sensing," *Chinese Phys. Lett.*, vol. 29, no. 10, 2012.

[14]   X. Wen, T. Ning, C. Li, Z. Kang, J. Li, H. You, T. Feng, J. Zheng, and W. Jian, "Liquid level measurement by applying the Mach–Zehnder interferometer based on up-tapers," *Appl. Opt.*, vol. 53, no. 1, p. 71, 2014.

[15]   T. Lu, Z. Li, D. Xia, K. He, and G. Zhang, "Asymmetric Fabry-Ṕrot fiber-optic pressure sensor for liquid-level measurement," *Rev. Sci. Instrum.*, vol. 80, no. 3, pp. 1–5, 2009.

[16]   C. W. Lai, Y. L. Lo, J. P. Yur, W. F. Liu, and C. H. Chuang, "Application of Fabry-Pérot and fiber Bragg grating pressure sensors to simultaneous measurement of liquid level and specific gravity," *Meas. J. Int. Meas. Confed.*, vol. 45, no. 3, pp. 469–473, 2012.

[17]   W. Wang and F. Li, "Large-range liquid level sensor based on an optical fibre extrinsic Fabry-Perot interferometer," *Opt. Lasers Eng.*, vol. 52, no. 1, pp. 201–205, 2014.

[18]   T. Guo, Q. Zhao, Q. Dou, H. Zhang, L. Xue, G. Huang, and X. Dong, "Temperature-Insensitive Fiber Bragg Grating Cantilever Beam," *IEEE Photonics Technol. Lett.*, vol. 17, no. 11, pp. 2400–2402, 2005.

[19]   M. G. Xu, L. Reekie, Y. T. Chow, and J. P. Dakin, "Optical in-fibre grating high pressure sensor," *Electron. Lett.*, vol. 29, no. 4, pp. 398–399, 1993.

[20]   Q. Jiang, "Hydraulic pressure sensor based on fiber Bragg grating," *Opt. Eng.*, vol. 50, no. 6, p. 64401, 2011.

[21]   O. F. Ameen, M. H. Younus, M. S. Aziz, A. I. Azmi, R. K. Raja Ibrahim, and S. K. Ghoshal, "Graphene diaphragm integrated FBG sensors for simultaneous measurement of water level and temperature," *Sensors Actuators, A Phys.*, vol. 252, pp. 225–232, 2016.

[22]   H. Ahmad, S. W. Harun, W. Y. Chong, M. Z. Zulkifli, Z. Yusof, and P. Poopalan, "High-sensivity pressure sensor using a polymer-embedded FBG," *Microw. Opt. Technol. Lett.*, vol. 50, no. 1, pp. 60–61, 2008.

[23]   Y. Liu, Z. Guo, Y. Zhang, K. S. Chiang, and X. Dong, "Simultaneous pressure and temperature measurement with polymer-coated fibre Bragg grating," *Eletronic Lett.*, vol. 36, no. 6, pp. 564–566, 2000.

[24]   D. Sengupta and P. Kishore, "Continuous liquid level monitoring sensor system using fiber Bragg grating," *Opt. Eng.*, vol. 53, no. 1, p. 17102, 2014.

[25]   D. Song, "Liquid-level sensor using a fiber Bragg grating and carbon fiber composite diaphragm," *Opt. Eng.*, vol. 50, no. 1, p. 14401, 2011.

[26]   P. F. C. C. Antunes, M. F. F. Domingues, N. J. Alberto, and P. S. André, "Optical Fiber Microcavity Strain Sensors Produced by the Catastrophic Fuse Effect," *IEEE Photonics Technol. Lett.*, vol. 26, no. 1, pp. 78–81, 2014.

[27]   K. O. Hill and G. Meltz, "Fiber Bragg grating technology fundamentals and overview," *J. Light. Technol.*, vol. 15, no. 8, pp. 1263–1276, 1997.

[28]   M. F. Domingues, C. A. Rodriguez, J. Martins, C. Tavares, C. Marques, N. Alberto, P. André, and P. Antunes, "Cost-effective optical fiber pressure sensor based on intrinsic Fabry-Perot interferometric micro-cavities," *Opt. Fiber Technol.*, vol. 42, no. February, pp. 56–62, 2018.

[29]   V. R. Machavaram, R. A. Badcock, and G. F. Fernando, "Fabrication of intrinsic fibre Fabry-Perot sensors in silica fibres using hydrofluoric acid etching," *Sensors Actuators, A Phys.*, vol. 138, no. 1, pp. 248–260, 2007.

[30]   T. Wei, Y. Han, H.-L. Tsai, and H. Xiao, "Miniaturized fiber inline Fabry-Perot interferometer fabricated with a femtosecond laser.," *Opt. Lett.*, vol. 33, no. 6, pp. 536–538, 2008.

[31]   Q. Shi, F. Lv, Z. Wang, L. Jin, J. J. Hu, Z. Liu, G. Kai, and X. Dong, "Environmentally Stable Fabry – Pérot-Type Strain Sensor Based On Hollow-Core Photonic Bandgap Fiber," *IEEE Photonics Technol. Lett.*, vol. 20, no. 4, pp. 2007–2009, 2008.

[32]   J. Ma, J. Ju, L. Jin, W. Jin, and D. Wang, "Fiber-tip micro-cavity for temperature and transverse load sensing," *Opt. Express*, vol. 19, no. 13, pp. 12418–12426, 2011.

[33]   M. De Fátima F.domingues, T. De Brito Paixão, E. F. T. Mesquita, N. Alberto, A. R. Frias, R. A. S. Ferreira, H. Varum, P. F. Da Costa Antunes, and P. S. De Brito André, "Liquid hydrostatic pressure optical sensor based on micro-cavity produced by the catastrophic fuse effect," *IEEE Sens. J.*, vol. 15, no. 10, pp. 5654–5658, 2015.

[34]   E. Hecht, *Optics*, 4th Intern. San Francisco: Addison-Wesley, 2002.

[35]   F. Domingues, A. R. Frias, P. Antunes, A. O. P. Sousa, R. A. S. Ferreira, and P. S. André, "Observation of the fuse effect discharge zone nonlinear velocity regime in erbium-doped fibres," *Electron. Lett.*, vol. 48, p. 1245, 2012.

[36]   M. F. Domingues, P. Antunes, N. Alberto, A. R. Frias, A. R. Bastos, R. A. S. Ferreira, and P. S. André, "Enhanced sensitivity high temperature optical fiber FPI sensor created with the catastrophic fuse effect," *Microw. Opt. Technol. Lett.*, vol. 57, no. 4, pp. 2781–2784, 2015.

[37]   C. A. F. Marques, G.-D. Peng, and D. J. Webb, "Highly sensitive liquid level monitoring system utilizing polymer fiber Bragg gratings," *Opt. Express*, vol. 23, no. 5, p. 6058, 2015.